Inorg. Chem. **2008**, *47*, 1648−1652

Inorganic Chemistry

Article

$Ba_2F_2Fe^{2+}{}_{0.5}Fe^{3+}S_3$: A Two-Dimensional Inhomogeneous Mixed Valence Iron Compound

Houria Kabbour* and Laurent Cario*

Institut des Matériaux Jean Rouxel (IMN), Université de Nantes, CNRS, 2 rue de la Houssinière
B.P. 32229, 44322 Nantes Cedex 3, France

Received October 12, 2007

The structure of the new mixed valence compound $Ba_2F_2Fe_{1.5}S_3$ was solved by means of single crystal X-ray analysis. It crystallizes in an orthorhombic cell, in the *Pnma* space group with the cell parameters $a = 12.528(3)$ Å, $b = 18.852(4)$ Å, and $c = 6.0896(12)$ Å. The structure is formed by the alternated stacking of fluorite type $[Ba_2F_2]^{2+}$ blocks and the newly discovered $[Fe_{1.5}S_3]^{2-}$ blocks. This $[Fe_{1.5}S_3]^{2-}$ block exhibits a mixed valence of iron with Fe(+II) located in octahedrons and Fe(+III) in tetrahedrons. Preliminary susceptibility measurements suggest a low dimensional antiferromagnetic behavior.

Introduction

Mixed valence compounds have always been of great importance in solid state sciences as they present very often unusual properties. In rare earth compounds, mixed valence can be associated to valence fluctuation[1] or heavy fermion[2] behavior. In conducting mixed valence transition metal oxides, charge ordering leads to metal insulator transition (MIT). For instance, the charge ordering of the manganese atoms in manganites of the perovskite type structure induces an MIT and leads to the well-known colossal magnetoresistance (CMR) observed in these systems.[3,4] For the same reason, the mixed valence magnetite has been a base model for solid state physics over decades. This compound exhibits ferromagnetic behavior at ambient temperature and a metal−insulator transition (the Verwey transition) at 120 K related to the localization of the conducting electrons in a regular array.[5–7]

In the last decades, the search for new iron compounds exhibiting a mixed valence, intrinsic or induced by doping, led to the discovery of interesting magnetic and/or electrical behaviors. For example, the mixed valence Fe_2OBO_3[8] compound shows an electrostatically driven charge ordering below 317 K. The mixed valence $Ba_6Fe_8S_{15}$[9] compound exhibits a spin-glass like behavior, and LaOFeP[10] shows superconductivity when a sufficient amount of Fe^{3+} is created upon substitution of fluorine to oxygen.

Here, we report on the discovery of a new mixed valence iron compound $Ba_2F_2Fe^{2+}{}_{0.5}Fe_1{}^{3+}S_3$. This compound exhibits a new structure type showing a striking $[Fe_{1.5}S_3]^{2-}$ layer in which Fe^{2+} are located in octahedral sites and Fe^{3+} in tetrahedral sites. Preliminary magnetic measurements suggest a low dimensional antiferromagnetic coupling of the iron ions.

Experimental Methods

Synthesis. $Ba_2F_2Fe_{1.5}S_3$ was synthesised using the classical high temperature ceramic method in an evacuated and flame-sealed silica tube. The solid reactants BaF_2, BaS, Fe, and S were mixed in stoechiometric proportions and ground in a mortar under Argon atmosphere. The resulting powder was subsequently pressed into a pellet and placed in an alumina crucible to avoid reactions with the tube. The mixture was then heated up to 800°C using a ramp of 50 °C/h, maintained at this temperature for 12 h, and cooled down at room temperature using a rate of 100°C/h. In order to

---

* To whom correspondence should be addressed. E-mail: h.kabbour@fkf.mpg.de (H.K.), laurent.cario@cnrs-imn.fr (L.C.).

(1) Berkooz, O. *J. Phys. Chem. Solids* **1969**, *30*, 1763.
(2) Steglich, F.; Geibel, C.; Gloos, K.; Olesch, G.; Schank, C.; Wassilew, C.; Loidl, A.; Krimmel, A.; Stewart, G. R. *J. Low Temp. Phys.* **1994**, *95*, 3–22.
(3) Imada, M. *Rev. Mod. Phys.* **1998**, *70*, 1039.
(4) Rao, C. N. R.; Cheetham, A. K. *Adv. Mater.* **1997**, *9*, 1009–1017.
(5) Verwey, E. J. W. *Nature* **1939**, *144*, 327–328.
(6) Verwey, E. J. W.; Haayman, P. W. *Physica* **1941**, *8*, 979.
(7) Verwey, E. J. W.; Haayman, P. W.; Romeijn, F. C. *J. Chem. Phys.* **1947**, *15*, 181.
(8) Attfield, J. P.; Bell, A. M. T.; Rodriguez-Martinez, L. M.; Greneche, J. M.; Cernik, R. J.; Clarke, J. F.; Perkins, D. A. *Nature* **1998**, *396*, 655–658.
(9) Gönen, Z. S.; Fournier, P.; Smolyaninova, V.; Greene, R.; Araujo-Moreira, F. M.; Eichhorn, B. *Chem. Mater.* **2000**, *12*, 3331–3336.
(10) Kamihara, Y.; Hiramatsu, H.; Hirano, M.; Kawamura, R.; Yanagi, H.; Kamiya, T.; Hosono, H. *J. Am. Chem. Soc.* **2006**, *128*, 10012–10013.

10.1021/ic702021s CCC: $40.75

Table 1. Cristallographic Data and Refinement Results for the Compound $Ba_2F_2Fe_{1.5}S_3$

Cristallographic and Physical Data	
chemical formulation	$Ba_2F_2Fe_{1.5}S_3$
molar mass (g•mol^{-1})	492.64
symmetry	orthorhombic
color	black
space group	*Pnma*
a (Å)	12.528(3)
b (Å)	18.852(4)
c (Å)	6.0896(12)
volume (Å^3)	1438.3(5)
Z	8
density (g cm^{-3})	4.55
crystal dimensions (μm)	50 × 5 × 50
Data Collection and Reduction	
temperature (K)	293(2)
wavelength (Å)	0.71073
F(000)	1736
angular range in θ (deg)	5.15–30.00
h, k, l ranges	$-17 < h < 14$; $-26 < k < 26$; $-8 < l < 7$
collected reflections	18118
independent reflections	2147
observed reflections ($I > 2\sigma(I)$)	1247
absorption correction	analytical
absorption coefficient (mm^{-1})	14.592
R_{int}	0.0601
T_{min}/T_{max}	0.493/0.927
Structural Refinement	
refinement method	least square on F^2
data/restrictions/parameters	2147/0/76
reliability factors	$R_{obs} = 0.0267$; $R_{all} = 0.0627$
weighted reliability factors	$R_{wobs} = 0.0455$; $R_{wall} = 0.0507$
S	0.961
residual electronic density (e$^-$/Å^3)	1.33/−1.45

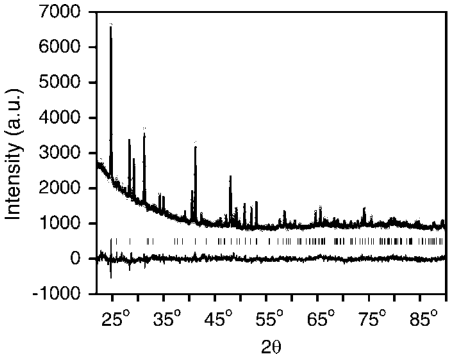

Figure 1. Experimental X-ray diffraction powder pattern of $Ba_2F_2Fe_{1.5}S_3$ (black circles). The black line corresponds to the calculated intensities obtained with the Rietveld method using the single crystal structure ($R_{bragg} = 7.23\%$, $R_p = 3.13\%$). The bottom curve is the difference between the experimental and calculated intensities, and the small marks indicate the Bragg peak positions.

improve its purity and homogeneity, the resulting product was reground in Argon atmosphere before applying a second heat treatment at the same temperature. A heat treatment of the so formed powder at 1000 °C for 12 h led to a congruent fusion which resulted in the formation of large black single crystals.

Chemical Analysis. This process was performed using a scanning electron microscope JEOL 5800LV equipped with an EDX (energy dispersive analysis of X-ray) apparatus. The analysis of the crystals indicated the presence of the four elements Ba, Fe, S, and F. Fluorine could not be quantified with accuracy using this method; however, the ratio between the other elements allowed us to calculate the formulation considering the charge neutrality. Ba, Fe, and S were found to be in the following proportions: 31.7%, 23.1%, and 45.7% respectively. These values compare well with the theoretical ratios expected from the formulation $Ba_2F_2Fe_{1.5}S_3$ (30.8%, 23.1%, and 46.1% for Ba, Fe, and S, respectively).

X-ray Single Crystal Diffraction. A single crystal of $Ba_2F_2Fe_{1.5}S_3$ was mounted on a capillary for this analysis. The X-ray diffraction data were collected on a Kappa CCD-NONIUS diffractometer using Mo Kα radiation (λ= 0.71073 Å). A set of 258 frames was collected in ϕ and ω scans mode, with a rotation of 1.4° and an exposure time of 140 s per frame; the crystal-to-detector distance was 36.4 mm. The absorption correction was applied using an analytical method taking in account the crystal dimensions by face indexation. Secondary extinctions and Lorentz-polarization correction were also applied. The initial set of 18118 reflections was averaged according to the *mmm* point group leading to 2147 independent reflections (= all data), with $R_{int} = 0.0601$. The data revealed an orthorhombic symmetry with cell parameters a = 12.528(3) Å, b = 18.852(4) Å, and c = 6.0896(12) Å, and systematic absences were consistent with space groups *Pnma*and $Pn2_1a$. SHELXTL[11] software was used for direct methods and structural refinement. Refinements in the space group *Pnma* produced a better result than with space group $Pn2_1a$. All atoms were refined with anisotropic displacements (except fluorine), and the structure converged with satisfying reliability factors (R_{obs} = 0.0267, R_{wobs} = 0.0455 for 1247 observed reflections ($I > 2\sigma(I)$) and 76 parameters). Details about the data collection and refinement are given in Table 1.

X-ray Powder Diffraction. XRPD was carried out on a position-sensitive detector diffractometer (INEL CPS120) using the Cu $K_{\alpha 1}$ radiation ($\lambda K_{\alpha 1}$= 1.540598 Å). A silica capillary was loaded with the powder sample in a glove box to avoid any contact with air. The data collection was then performed in the 20–90° 2θ range at room temperature. The resulting powder pattern did not show any evidence of known major phases or impurities. The Jana2006 chain program[12] was used to calculate the theoretical powder pattern of $Ba_2F_2Fe_{1.5}S_3$ using as structural model the structure refined from the single crystal study. The calculated powder pattern was then compared to the experimental one (i.e., we performed a Rietveld refinement with all structural parameters fixed to the single crystal values).

Susceptibility Measurements. A powder sample (m = 123.5 mg) was used for these mesaurements using a Quantum Design MPMS SQUID magnetometer under an applied field of 1000 G and in the temperature range 30–300 K. Zero field cooled and field cooled data were corrected from the sample holder contribution and the core electrons diamagnetism.

Results and Discussion

A great number of mixed anions systems reported so far such as rare earth or alkaline earth transition metal oxychalcogenides[13–15] and oxypnictides[16,17] show layered-type in-

---

(11) Sheldrick, G. M. *SHELXL97*; University of Göttingen: Germany, 1997.

(12) Petricek, V.; Dusek, M.; Palatinus, L. *The crystallographic computing system JANA 2006*, beta version; Academy of Science of Czeck Republic: Praha, 2006.

(13) Goga, M.; Seshadri, R.; Ksenofontov, V.; Gütlich, P.; Tremel, W. *Chem. Commun.* **1999**, 979–980.

(14) Boyer, C.; Deudon, C.; Meerschaut, A. *C.R. Acad. Sci. Paris* **1999**, *serie II c*, 93–99.

(15) Otzschi, K.; Ogino, H.; Shimoyama, J. I.; Kishio, K. *J. Low Temp. Phys.* **1999**, *117*, 729–733.

(16) Ozawa, T. C.; Kauzlarich, S. M. *Chem. Mater.* **2001**, *13*, 1804–1810.

(17) Nientiedt, A. T.; Jeitschko, W. *Inorg. Chem.* **1998**, *37*, 386–389.

Table 2. Atomic Positions and Isotropic Displacement Parameters (or Equivalents) in $Ba_2F_2Fe_{1.5}S_3$

atom	site	*X*	*y*	*z*	$U_{iso/eq*}$ (Å^2)
Ba1	*8d*	0.25191(4)	0.92103(3)	0.23501(3)	0.0082(1)*
Ba2	*8d*	0.99772(4)	0.92080(3)	0.75586(3)	0.0080(1)*
Fe1	*4c*	0.29724(6)	0.7500	0.85647(12)	0.0083(2)*
Fe2	*4c*	0.45159(6)	0.7500	0.36111(12)	0.0083(2)*
Fe3	*4c*	0.12492(8)	0.7500	0.49676(15)	0.0180(2)*
S1	*4c*	0.2783(3)	0.7500	0.2315(2)	0.0082(6)*
S2	*8d*	0.7727(2)	0.15123(11)	0.2800(2)	0.0132(4)*
S3	*8d*	0.9768(2)	0.15135(12)	0.7263(2)	0.0133(4)*
S4	*4c*	0.9711(3)	0.7500	0.7644(2)	0.0093(6)*
F1	*8d*	0.8745(4)	0.99823(10)	1.0105(8)	0.0110(5)
F2	*8d*	0.3750(4)	0.99936(10)	0.9914(9)	0.0120(5)

Table 3. Anisotropic Displacement Parameters in $Ba_2F_2Fe_{1.5}S_3$

atom	U11	U22	U33	U12	U13	U23
Ba1	0.0088(2)	0.0086(3)	0.0072(1)	0.0001(2)	0.00003(9)	0.0006(1)
Ba2	0.0078(2)	0.0089(3)	0.0073(1)	0.0017(2)	−0.00014(6)	−0.0009(1)
Fe1	0.0086(4)	0.0088(5)	0.0074(4)	0	0.0005(3)	0
Fe2	0.0083(4)	0.0097(5)	0.0069(4)	0	−0.0004(3)	0
Fe3	0.0168(4)	0.0167(4)	0.0204(4)	0	0.0088(3)	0
S1	0.0059(12)	0.0118(15)	0.0069(7)	0	−0.0009(5)	0
S2	0.0143(8)	0.0140(9)	0.0115(4)	0.0076(7)	0.0010(5)	0.0029(5)
S3	0.0144(8)	0.0151(9)	0.0105(5)	−0.0047(7)	0.0009(5)	−0.0034(5)
S4	0.0099(13)	0.0109(15)	0.0071(7)	0	0.0002(5)	0

tergrowth structures. During the last three years, we have taken into good account this feature to develop the concept of layered secondary building units (2D SBU) and design new inorganic mixed anions compounds with intergrowth structures.[18] Hence, we could predict the structures of a whole family of compounds from the stacking of 2D SBU of the fluorite type $[Ba_2F_2]^{2+}$ alternating regularly with other type of 2D SBU.[18–22] One of these compounds, namely $Ba_2F_2Fe_2OS_2$, contains a striking Fe_2OS_2 2D SBU with a Fe_2O square plane.[23] In an attempt to introduce a mixed valence Fe^{2+}/Fe^{3+} in this compound, we have obtained the title compound as a side product. Subsequently, a single phase sample of $Ba_2F_2Fe_{1.5}S_3$ was synthesised as described in the experimental section. The X-ray powder diffraction pattern (see Figure 1) showed no hint of known phase and could not be indexed with the standard JCPDS database. The structure of $Ba_2F_2Fe_{1.5}S_3$ was solved using single crystal X-ray analysis. The crystallographic data and the refinement results are given in Table 1. The atomic positions and isotropic (or equivalent) displacement parameters are presented in Table 2. The anisotropic displacement parameters are listed in Table 3.

Figure 2 shows the structure of $Ba_2F_2Fe_{1.5}S_3$ resulting from the stacking along the *b* axis of the 2D SBU, $[Ba_2F_2]^{2+}$ of the fluorite type, and $[Fe_{1.5}S_3]^{2-}$. In the former, the fluorine atoms within the block are surrounded by four barium cations, while the barium atoms are surrounded by four fluorine atoms and five sulphur atoms and are located at the interface between the two blocks.

Three different iron atoms sites are present within the $[Fe_{1.5}S_3]^{2-}$ block. Two of them (i.e. Fe1 and Fe2) are located in sulphur tetrahedrons with Fe−S distances ranging from 2.22 to 2.31 Å (see Table 4). The third iron atom (Fe3) occupies the center of a sulphur octahedron with Fe−S distances slightly higher than previously and in the range 2.51–2.64 Å (see Table 4). A projection of the block in the (*ac*) plane is shown in Figure 2b. The polyhedrons are all linked together by the edges. Along the *c* axis, the tetrahedrons form chains separated by octahedrons disconnected from each other. Figure 3 represents the individual environments of each cation (Ba, Fe1, Fe2, and Fe3), and Table 4 summarizes the main interatomic distances.

The structure of the sulfide block $[Fe_{1.5}S_3]^{2-}$ is new and cannot be related to any known structural type. However, it can be compared with other structures. Figure 4 compares the EuS layer within the misfit layer compound $[(EuS)_{1.5}]_{1.15}NbS_2$[24] (Figure 4a), the $SnTe_2$ layer in Ba_2SnTe_5[25] (Figure 4b), the inner atomic layer ($Fe_{1.5}S$) of the $[Fe_{1.5}S_3]^{2-}$ block projected in the (*ac*) plane (Figure 4c), and the Fe_2O layer in $Ba_2F_2Fe_2OS_2$ or $La_2O_2Fe_2OSe_2$[26] (Figure 4d). All layers can be described similarly on the basis of an anion squares network; however, distortions of this network and different cation/anion ratios lead to different cation environments (tetrahedrons or octahedrons). In the EuS layer (cation/anion ratio 1/1), the Eu atoms are located in the centers of the S squares which define the basal plane of a perfect octahedral environment. In the $SnTe_2$ layer (cation/anion ratio 1/2), the Sn atoms are shifted from the

---

(18) Cario, L.; Kabbour, H.; Meerschaut, A. *Chem. Mater.* **2005**, *17*, 234–236.

(19) Kabbour, H.; Cario, L.; Boucher, F. *J. Mater. Chem.* **2005**, *15*, 3525–3531.

(20) Kabbour, H.; Cario, L. *Inorg. Chem.* **2006**, *45*, 2713–2717.

(21) Kabbour, H.; Cario, L.; Danot, M.; Meerschaut, A. *Inorg. Chem.* **2006**, *45*, 917–922.

(22) Kabbour, H.; Cario, L.; Jobic, S.; Corraze, B. *J. Mater. Chem.* **2006**, *16*, 4165–4169.

(23) Kabbour, H.; Janod, E.; Corraze, B.; Danot, M.; Lee, C.; Whangbo, M.-H.; Cario, L. submitted.

(24) Cario, L.; Lafond, A.; Palvadeau, P.; Deudon, C.; Meerschaut, A. *J. Solid State Chem.* **1999**, *147*, 58–67.

(25) Li, J.; Liszewski, Y. Y.; Chen, L. A.; Mulley, S.; Proserpio, D. M. *Chem. Mater.* **1996**, *8*, 598–600.

(26) Mayer, J. M.; Schneemeyer, L. F.; Siegrist, T.; Waszczak, J. V.; Van Dover, R. B. *Angew. Chem., Int. Ed.* **1992**, *31*, 1645–1647.

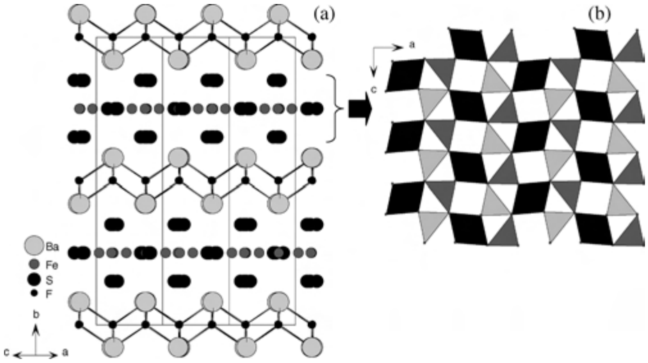

Figure 2. Cristalline Structure of the Compound $Ba_2F_2Fe_{1.5}S_3$ (a) and Projection of the $[Fe_{1.5}S_3]$ block in the (*ac*) plane (b).

Table 4. Interatomic Distances in the Compound $Ba_2F_2Fe_{1.5}S_3$

atom1−atom2	distance (Å)	atom1−atom2	distance (Å)
Ba1−F2	2.600 (4)	Fe1−S2	2.220 (2)
Ba1−F1	2.623 (4)	Fe1−S2	2.220 (2)
Ba1−F1	2.657 (4)	Fe1−S1	2.296 (2)
Ba1−F2	2.686 (4)	Fe1−S4	2.299 (4)
Ba1−S3	3.182 (2)	Fe2−S3	2.222 (2)
Ba1−S1	3.241 (1)	Fe2−S3	2.222 (2)
Ba1−S2	3.267 (2)	Fe2−S4	2.294 (2)
Ba1−S2	3.433 (2)	Fe2−S1	2.309 (3)
Ba1−S3	3.663 (3)	Fe3−S1	2.511 (3)
Ba2−F2	2.613 (4)	Fe3−S4	2.524 (3)
Ba2−F1	2.630(4)	Fe3−S3	2.632 (2)
Ba2−F1	2.630 (4)	Fe3−S3	2.632 (2)
Ba2−F2	2.721 (4)	Fe3−S2	2.638 (2)
Ba2−S2	3.188 (2)	Fe3−S2	2.638 (2)
Ba2−S4	3.238 (1)		
Ba2−S3	3.252 (2)		
Ba2−S3	3.449 (2)		
Ba2−S2	3.653 (2)		

centers of the distorted Te square and, therefore, occupy tetrahedron environments. In the Fe_2O layer (cation/anion ratio 2/1), the oxygen square network is perfectly symmetrical and the iron atoms are located on the square's edges in perfect oxygen octahedrons. As shown in Figure 4c, the $Fe_{1.5}S$ layer (cation/anion ratio 1.5/1) represents an arrangement at midway between the $SnTe_2$ and the Fe_2O layers. There are two types of iron cations: one decentered within the squares in a tetrahedral environment (like in $SnTe_2$) and one on the edges in an octahedral environment (like in Fe_2O).

A major issue for this compound concerns the oxidation state of iron. A simple calculation using the formulation $Ba_2F_2Fe_{1.5}S_3$ and assuming the following oxidation states: Ba(+II), F(−I), and S(−II), leads to a mixed valence Fe^{+II}/Fe^{+III} for the iron atoms. This is confirmed by bond valences calculations of cations using the Brown valence method.[27,28] We found oxidation states close to +III for Fe1 and Fe2 situated in tetrahedrons, and an oxidation state close to +II for Fe3 in an octahedral environment (exact values are reported in Table 5). Therefore, $Ba_2F_2Fe_{1.5}S_3$ can be considered as a new example of an inhomogeneous mixed valence iron compound.

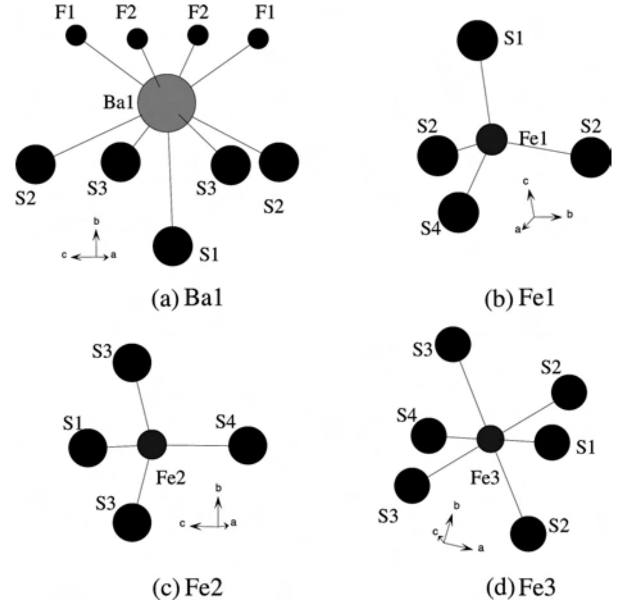

(a) Ba1 (b) Fe1 (c) Fe2 (d) Fe3

Figure 3. Cation environments in $Ba_2F_2Fe_{1.5}S_3$: Ba1 (a), Fe1 (b), Fe2 (c), and Fe3 (d).

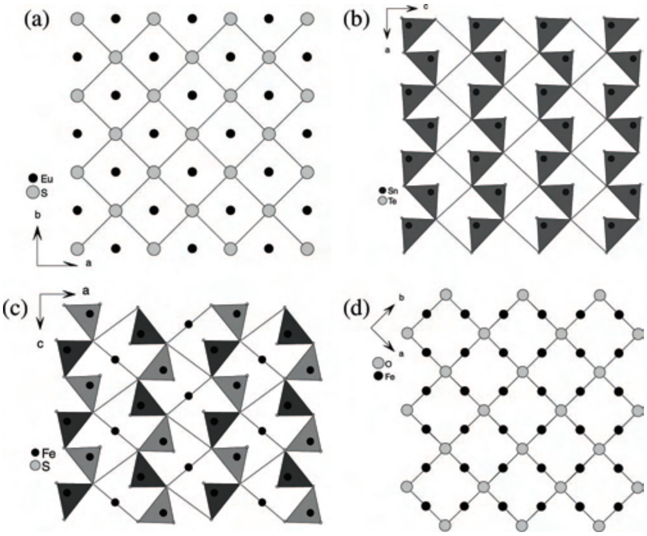

Figure 4. Comparison of the layer ($Fe_{1.5}S$) in $Ba_2F_2Fe_{1.5}S_3$ (c) with other (M/X) layers (M = Eu, Sn, or Fe and X = oxygen or chalcogene) from the 2D misfit $[(EuS)_{1,5}]_{1.15}NbS_2$ (a) and the compounds Ba_2SnTe_5 (b) and $Ba_2F_2Fe_2OS_2$ (d).

Table 5. Bond Valences in the Compound $Ba_2F_2Fe_{1.5}S_3$

atom	Ba1	Ba2	Fe1	Fe2	Fe3
valence[a]	2.31	2.30	3.08	3.06	1.87

[a] Calculated using the Brown method.

As a mixed valence of iron is often related to interesting magnetic properties, we have undertaken preliminary magnetic susceptibility measurements on a powder sample of $Ba_2F_2Fe_{1.5}S_3$. Rietveld analysis of the powder X-ray diffraction pattern confirmed that this sample is of good quality and exhibits the same structure as the crystals formed at higher temperature (see Figure 1). The temperature dependence of the magnetic susceptibility of this sample is represented in Figure 5. The zero field cooled and field cooled susceptibility curves show a small discrepancy. This discrepancy is likely related to the presence of an iron

---

(27) Brown, I. D. The bond valence method: an empirical approach to chemical structure and bonding. *Structure and Bonding in Crystals*; M. O'Keeffe, A. N. E., Ed. Academic Press: New York, 1981; Vol. *II*, pp 1–30.

(28) Brese, N. E.; O'Keeffe, M. *Acta Crystallogr., Sect. B* **1991**, *47*, 192–197.

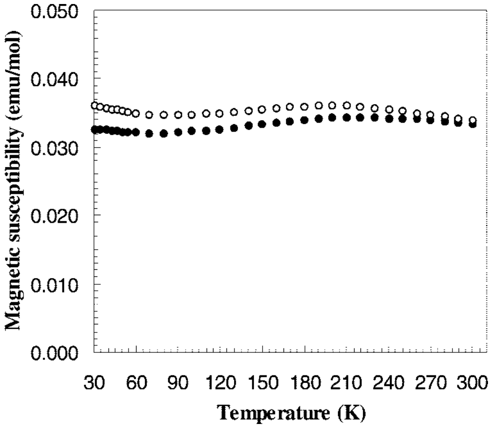

Figure 5. Magnetic susceptibility measured for $Ba_2F_2Fe_{1.5}S_3$: zero field cooled (black circles) and field cooled (empty circles) measurements in the temperature range 30–300 K.

sulphide impurity as several successive annealing treatments reduced its magnitude. Unfortunately, further annealing did not complete the removal of this impurity which is present in an amount barely detectable by powder X-ray analysis. Although our measurements are hampered by the magnetic contribution of this impurity, assumptions about the nature of the magnetic interactions occurring in $Ba_2F_2Fe_{1.5}S_3$ can be proposed. At high temperatures (≈200 K) the susceptibility shows a broad maximum. This particular curvature is encountered in materials where low dimensional antiferromagnetic interactions are present. For instance, such behavior has been previously reported in the layered intercalated $FePS_3$ compounds.[29] This low dimensional magnetic behavior matches well with the structure of the $Ba_2F_2Fe_{1.5}S_3$ compound. The piled up structure formed by a magnetic block $[Fe_{1.5}S_3]^{2-}$ alternating with a nonmagnetic block $[Ba_2F_2]^{2+}$ minimizes possible interaction along the *b* axis between iron atoms from different blocks. In that respect, 2D type magnetic interactions are the most likely to occur within the $Ba_2F_2Fe_{1.5}S_3$ compound.

Conclusion

We have synthesised and solved the structure of the new mixed valence compound $Ba_2F_2Fe_{1.5}S_3$. This compound crystallizes in a new structure type formed by the stacking of the well-known fluorite type block $[Ba_2F_2]^{2+}$ with the unknown block $[Fe_{1.5}S_3]^{2-}$. This $[Fe_{1.5}S_3]^{2-}$ block exhibits a mixed valence of iron with Fe(+II) in octahedrons and Fe(+III) in tetrahedrons. Preliminary susceptibility measurements suggest a low dimensional antiferromagnetic behavior.

Supporting Information Available: Crystallographic information file (CIF) of the compound $Ba_2F_2Fe_{1.5}S_3$. This material is available free of charge via the Internet at http://pubs.acs.org.

IC702021S

---

[29] Joy, P. A.; Vasudevan, S. *Chem. Mater.* **1993**, *5*, 1182–1191.